Supporting Information for:

Three-State Fluorescence Hydrochromism of a Fluorophore-Spacer-Receptor System with Variations in Relative Humidity

Yanhai Ni,[a] Yishan Han, [a] Evgeny A. Kataev*[b], and Mark A. Olson*[c]

[a] *Institute for Molecular Design and Synthesis, School of Pharmaceutical Science and Technology, Tianjin University, Tianjin, P. R. China.*
[b] *Department of Chemistry and Pharmacy, Friedrich Alexander University Erlangen-Nürnberg, Erlangen, Germany*
[c] *Department of Physical and Environmental Sciences, Texas A&M University Corpus Christi, Corpus Christi, Texas, USA.*

Table of Contents

1. General Methods

Starting materials and reagents were purchased from Tokyo Chemical Industry (TCI) and used as received. Analytical thin-layer chromatography (TLC) was performed on aluminum sheets, precoated with silica gel 60-F254 (Merck 5554). Deuterated solvents (Cambridge Isotope Laboratories) for NMR spectroscopic analyses were used as received. ^{1}H and ^{13}C NMR spectra were recorded on a Bruker Avance 400 MHz spectrometer. Chemical shifts are reported in ppm relative to the residual signal of the solvent ($CHCl_3$: δ 7.26 ppm for 1H and $CDCl_3$: δ 77.16 ppm). High resolution electrospray ionization (HR-ESI) mass spectral analyses were performed by the Bruker 1290 UPLC / micrOTOF-Q II. Solution UV-Vis absorption spectra were measured on a Hitachi U-3900 UV-Vis spectrometer with a 1 cm path length cuvette at 298 K. Fluorescence emission spectra in solution were recorded on an Edinburgh Instruments FLS980 time-resolved fluorescence spectrometer equipped with an integrating sphere. All solid-state emission spectra were recorded on an Ocean Optics QE65PRO fiber optic spectrometer. Solid-state absolute quantum yield was obtained on an Edinburgh Instruments FLS980 time-resolved fluorescence spectrometer equipped with an integrating sphere. Dynamic vapor sorption isotherms were recorded on a TA-Q5000SA. Chamber relative humidity was maintained using a Suzhou Furande Experimental Equipment Company humidity controller. Thermogravimetric analysis (TGA) was investigated by a TA instruments Q500 thermal analyzer and differential scanning calorimeter (DSC) was recorded by TA Instruments Q200 scanning calorimeter. The PXRD patterns were measured by using a Rigaku instruments MiniFlex600 X-ray diffractometer.

Photophysical Characterization as a Function of Relative Humidity for NIP·Br in the Solid State

For the measurement of variable humidity UV-Vis absorption and fluorescence emission spectra, a humidity chamber equipped with a dual gas/liquid mass flow controller was employed to regulate and maintain a constant humidity of 0 to 99% relative humidity using dry argon gas and a syringe pump equipped with a water containing syringe. Spectra was collected in-situ using an Ocean Optics QE65PRO fiber optic spectrometer and the average relative humidity during these experiments was monitored electronically using a DT-625 humidity/temperature sensor at a temperature of 25 ± 3 °C. Pristine powder samples of

NIP·Br was dried on a hot plate at 80 ºC for 30 minutes. At this time the relative humidity within the chamber was set to a desired level and allowed to equilibrate for 60 minutes. Samples were then immediately placed into the chamber and allowed to cool to room temperature prior to recording spectra. The UV light source was turned off after each spectral measurement in order to maintain a constant temperature within the chamber. Each incremental increase in the relative humidity was allowed to equilibrate for 60 minutes prior to spectral measurement. Each incremental decrease in the relative humidity was allowed to equilibrate for 90 minutes prior to spectral measurement on account of slower water desorption kinetics.

Thermal Gravimetric Analysis (TGA)

A sample of hydrate, **NIP**·Br·H_2O (5.74 mg, 10.38 μmol), which was prepared by setting a dry powdered sample into the 80% relative humidity chamber for 12 hours, was placed inside a platinum vessel and heated under continuous air flow (60.0 mL/min) from 20 ℃ to 115 ℃ at a rate of 10 ℃/min. The temperature was then allowed to cool to room temperature.

Differential Scanning Calorimetry Analysis (DSC)

A sample of hydrate, **NIP**·Br·H_2O (5.4 mg, 9.8 μmol), was enclosed inside a Tzero aluminum vessel and heated under continuous nitrogen flow (50 mL/min) from 20 ℃ to 115 ℃ at a rate of 10 ℃/min. The temperature was then allowed to cool to room temperature.

Powder X-Ray Diffraction Analysis (PXRD)

PXRD diffractograms were obtained using 100 mg of anhydrate (**NIP**·Br), hydrate (**NIP**·Br·H_2O), and solvate (**NIP**·Br·nH_2O). The samples were scanned from 5 to 40 degree at a rate of 4 degrees per minute.

2. Synthesis of NIP·Br

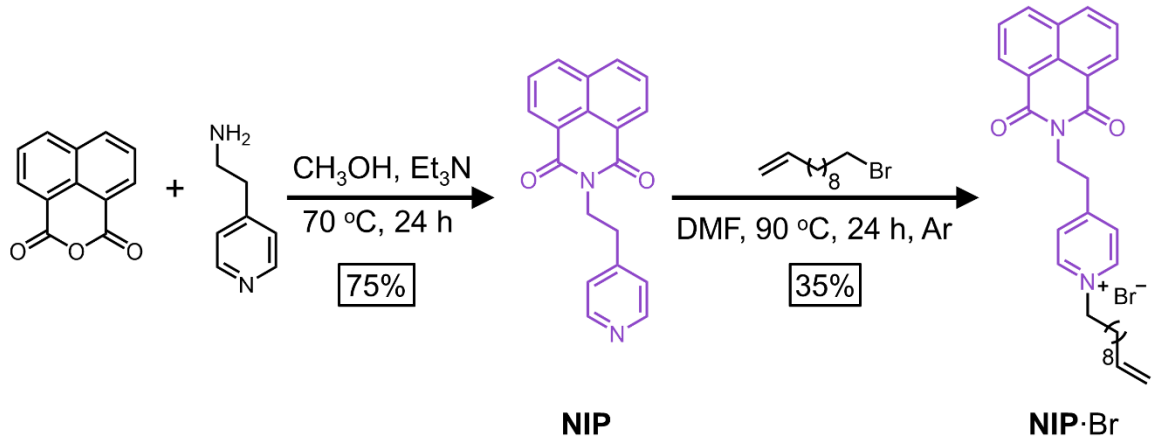

Scheme S1. The synthesis of the NI-pyridinium-based integrated fluorophore-spacer-receptors, **NIP**·Br.

NIP: 1,8-naphthalic anhydride (5.0 g, 25.3 mmol) was dissolved in methanol (100 mL) at room temperature, then 4-pyridylethylamine (3.4 g, 27.8 mmol) was added to the solution. Triethylamine (0.5 mL) was added to the reaction mixture as the catalyst. The reaction mixture was heated at 80 ℃ for 24 hours. The reaction mixture was then cooled to room temperature and stirred for further 30 minutes. The precipitate was filtered, washed with methanol, and dried under vacuum. The product **NIP** (5.7 g, 75%) was obtained as a light yellow powder. Mp: 181.2 ± 0.5 ℃. IR (KBr): 1695 and 1655 [ν N(C=O)$_2$], 1342 [ν CN], 782 [δ ArH]. ^{1}H NMR (400 MHz, $CDCl_3$, 25 °C): δ = 8.60 (dd, *J* = 7.3, 1.1 Hz, 2H), 8.52 (dd, *J* = 4.4, 1.6 Hz, 2H), 8.23 (dd, *J* = 8.3, 1.0 Hz, 2H), 7.81-7.74 (m, 2H), 7.29 (dd, *J* = 4.5, 1.5 Hz, 2H), 4.47-4.40 (m, 2H), 3.10-3.00 (m, 2H). ^{13}C NMR ($CDCl_3$, 101 MHz, 25 °C): δ = 33.48, 40.48, 122.26, 124.29, 126.91, 127.94, 131.20, 131.46, 134.06, 147.64, 149.83, 163.84. HRMS (ESI): m/z calcd for $C_{19}H_{14}N_2O_2$: 325.0947; found: 325.0961 [M+Na].

NIP·Br: 2-(2-(pyridin-4-yl)ethyl)-1H-benzo[de]isoquinoline-1,3(2H)-dione **NIP** (1.1 g, 3.6 mmol) was added to a 100 mL 3-neck flask under an argon atmosphere and dry degassed DMF (20 mL) was added to the flask under argon. 11-bromo-1-undecene (1.02 g, 4.38 mmol) was added dropwise into the mixture within 30 minutes while the solution of 2-(2-(pyridin-4-yl)ethyl)-1H-benzo[de]isoquinoline -1,3(2H)-dione **NIP** was stirred at 90 ℃, then the reaction mixture was allowed stir at 90 ℃ under argon for 24 hours. The reaction mixture was then cooled to room temperature and the solvent was evaporated in vacuum. Further purification by column chromatography (SiO_2, 3% MeOH in DCM) afforded **NIP**·Br (0.7 g, 35%) as a yellow solid. Mp: 158.6 ± 0.5 ℃. IR (KBr): 1702 and 1660 [ν N(C=O)$_2$], 1640 [ν C=C], 1346 [ν CN],

779 [δ ArH]. ^{1}H NMR (400 MHz, $CDCl_3$, 25 °C): δ = 9.35 (d, *J* = 6.3 Hz, 2H), 8.52 (dd, *J* = 7.3, 1.0 Hz, 2H), 8.23 (dd, *J* = 8.3, 0.9 Hz, 2H), 7.95 (d, *J* = 6.1 Hz, 2H), 7.74 (dd, *J* = 8.2, 7.4 Hz, 2H), 5.78 (ddt, *J* = 16.9, 10.2, 6.7 Hz, 1H), 5.03-4.85 (m, 4H), 4.52 (t, *J* = 7.2 Hz, 2H), 3.34 (t, *J* = 7.2 Hz, 2H), 2.01 (td, *J* = 6.7, 1.3 Hz, 4H), 1.39-1.17 (m, 12H). ^{13}C NMR ($CDCl_3$, 101 MHz, 25 °C): δ = 25.96, 28.80, 28.99, 29.05, 29.28, 29.31, 31.86, 33.70, 34.25, 39.39, 61.29, 114.12, 121.78, 126.99, 127.92, 128.53, 131.41, 131.51, 134.51, 139.08, 144.75, 159.05, 163.83. HRMS (ESI): m/z calcd for $C_{30}H_{35}N_2O_2$: 455.2693; found: 455.2714 $[M\text{-}Br]^+$.

3. NMR Spectroscopic Characterization Data

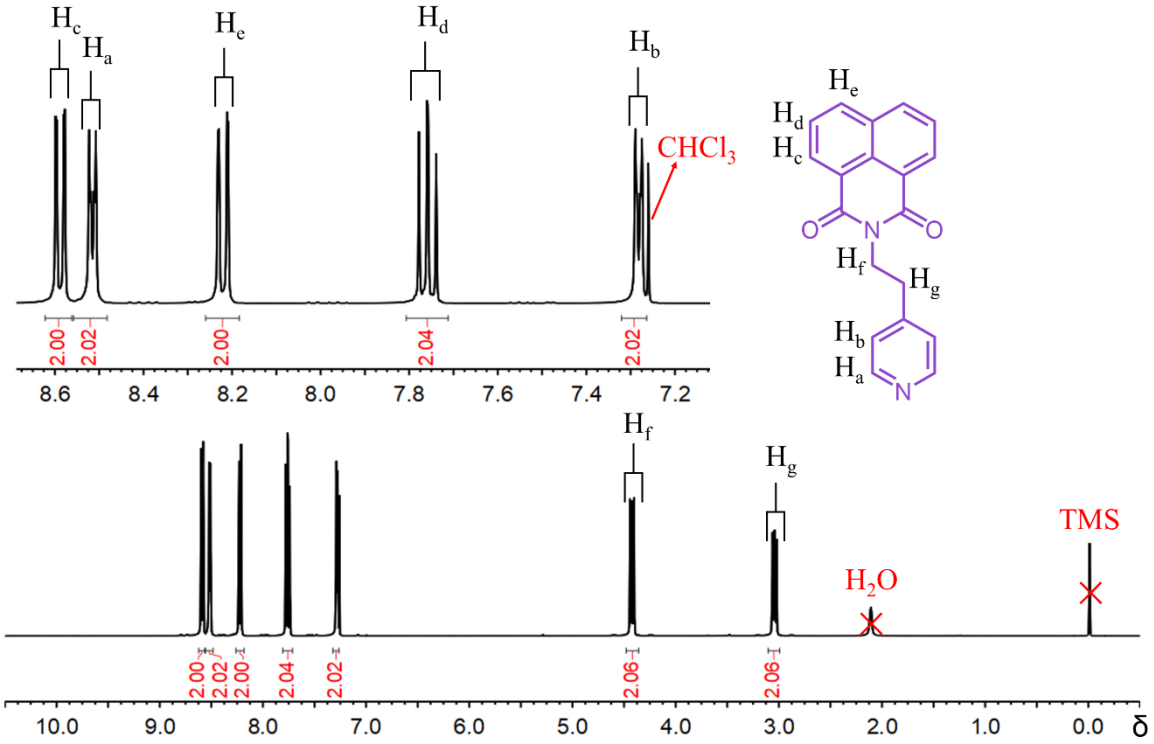

Figure S1. ^{1}H NMR spectrum of **NIP** (400 MHz, $CDCl_3$, 298 K).

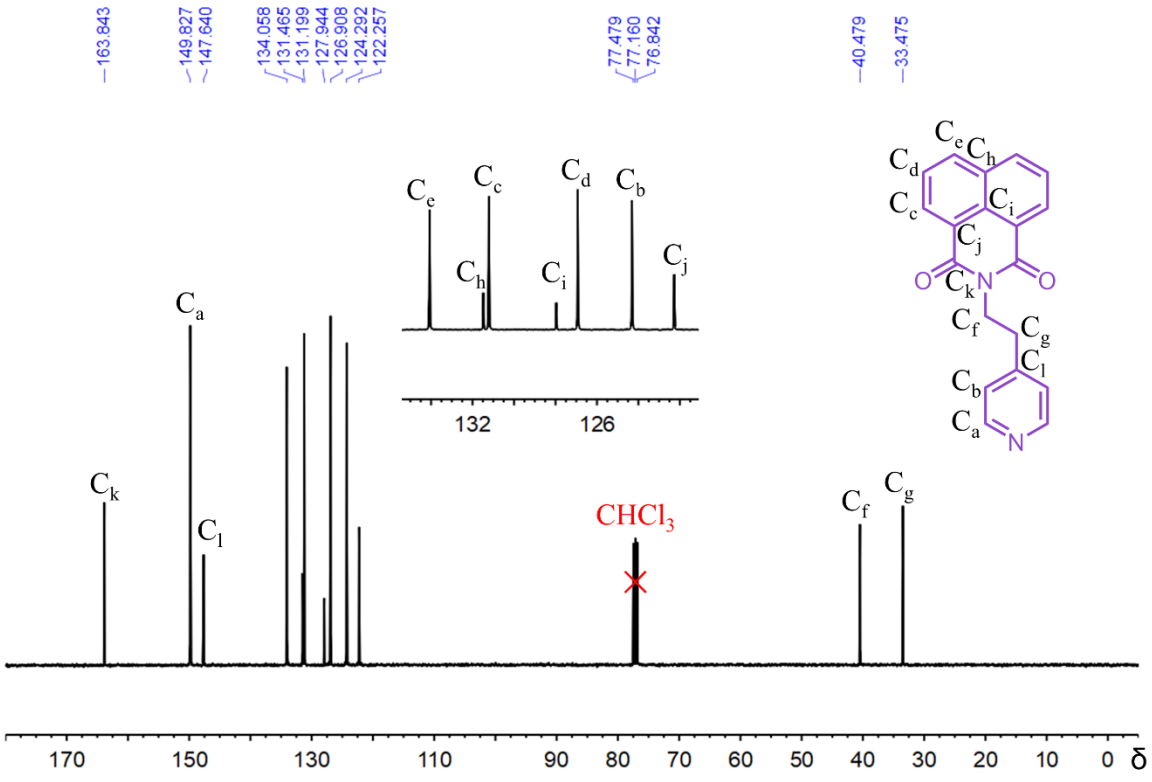

Figure S2. ^{13}C NMR spectrum of **NIP** (101 MHz, $CDCl_3$, 298 K).

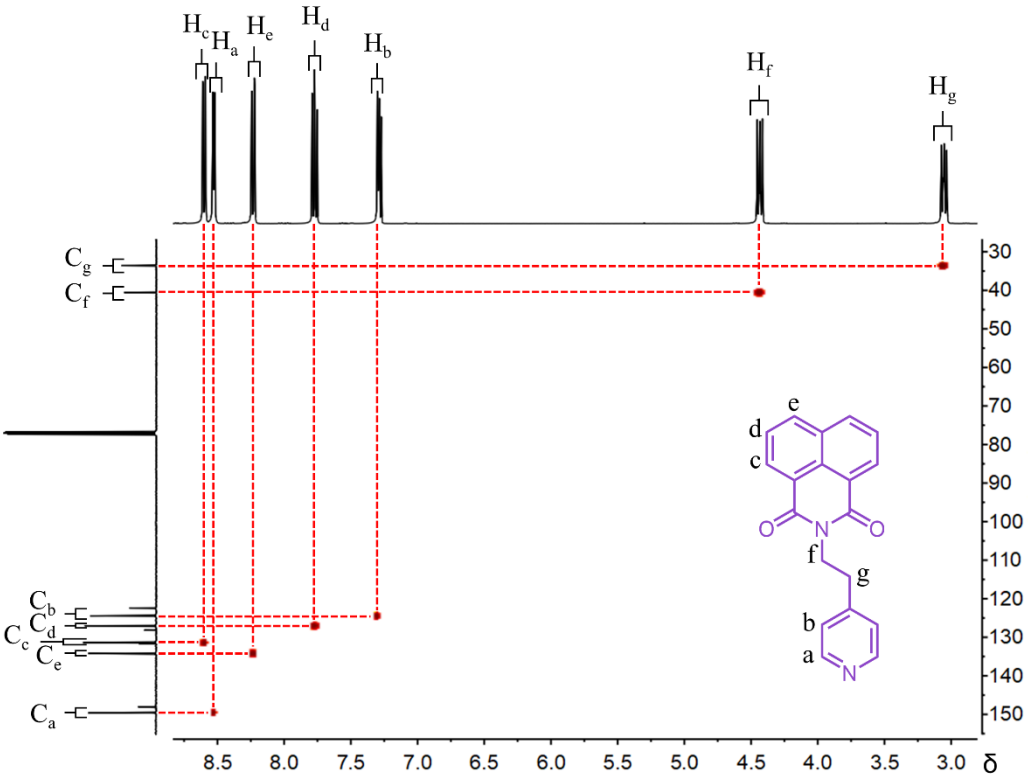

Figure S3. HSQC NMR spectrum of **NIP** (400 MHz, $CDCl_3$, 298 K).

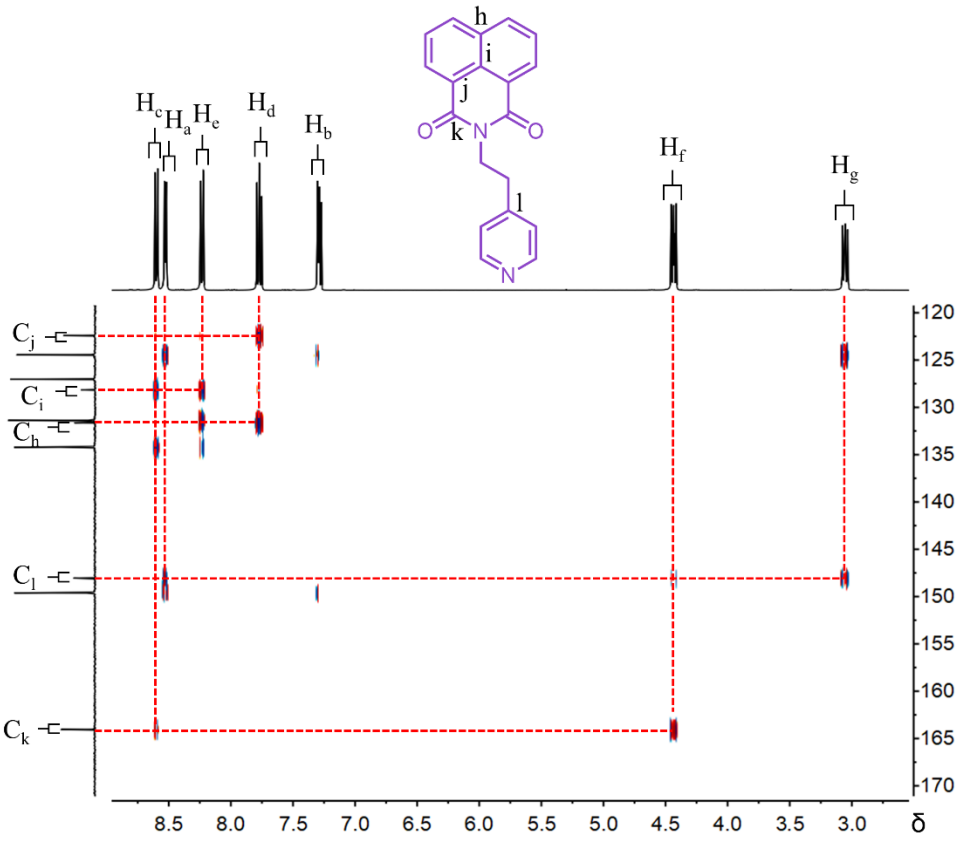

Figure S4. HMBC NMR spectrum of **NIP** (400 MHz, $CDCl_3$, 298 K).

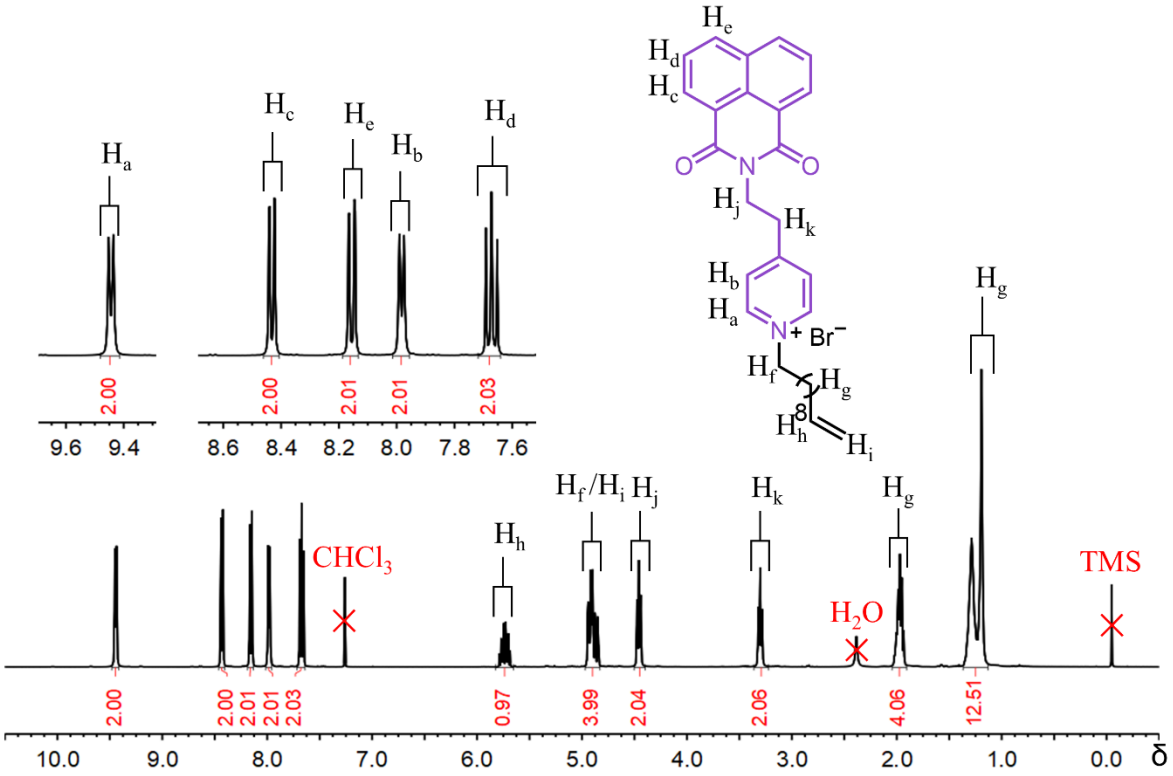

Figure S5. ^{1}H NMR spectrum of **NIP**·Br (400 MHz, $CDCl_3$, 298 K).

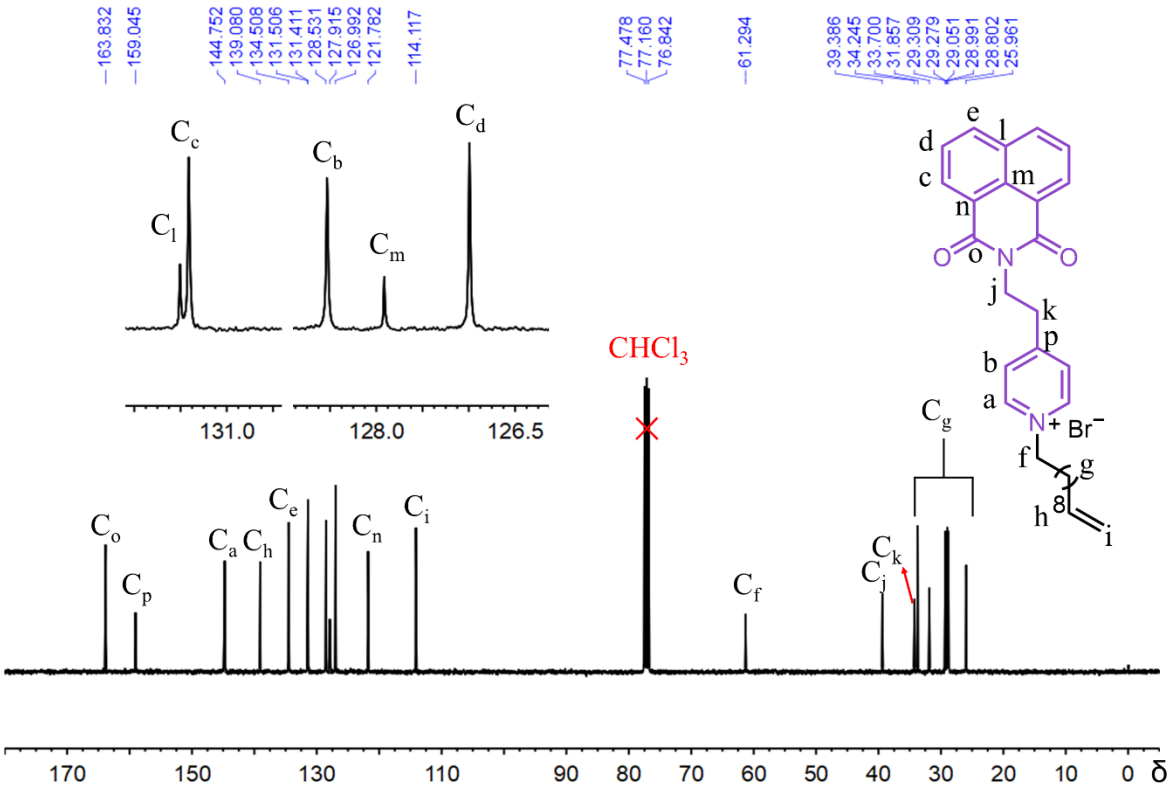

Figure S6. ^{13}C NMR spectrum of **NIP**·Br (101 MHz, $CDCl_3$, 298 K).

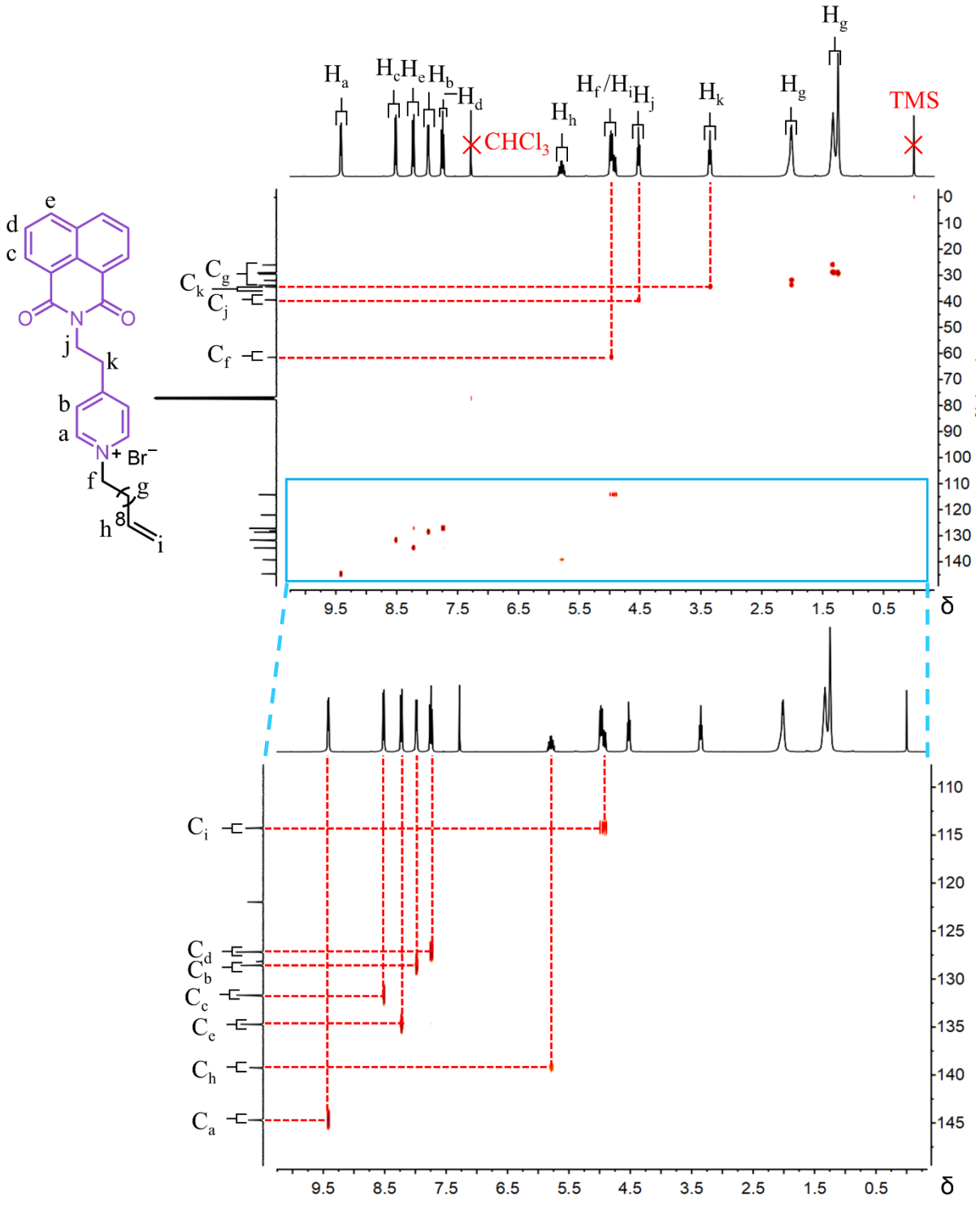

Figure S7. HSQC NMR spectrum of **NIP**·Br (400 MHz, $CDCl_3$, 298 K).

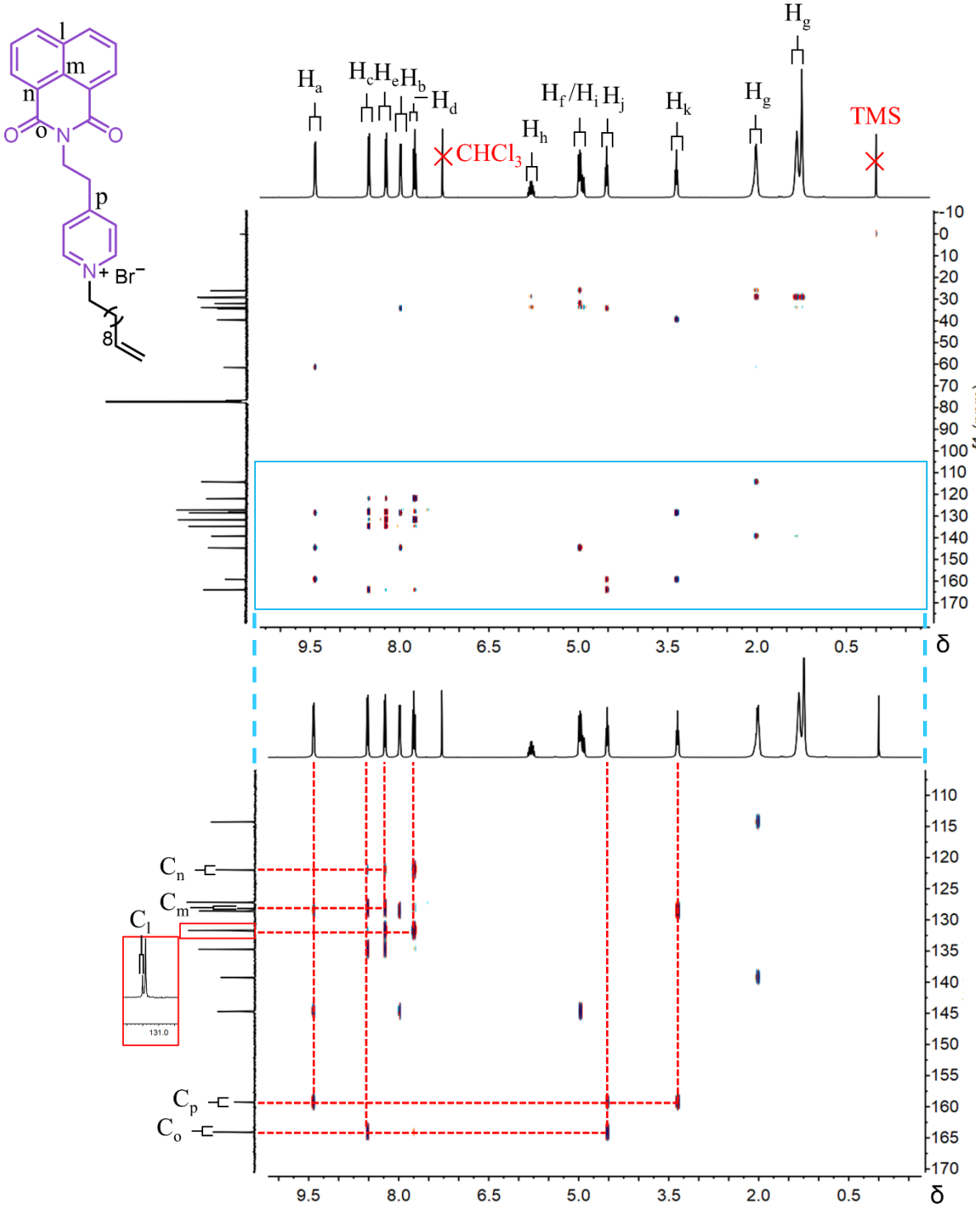

Figure S8. HMBC NMR spectrum of **NIP**·Br (400 MHz, $CDCl_3$, 298 K).

4. High Resolution Mass Spectrometry Data

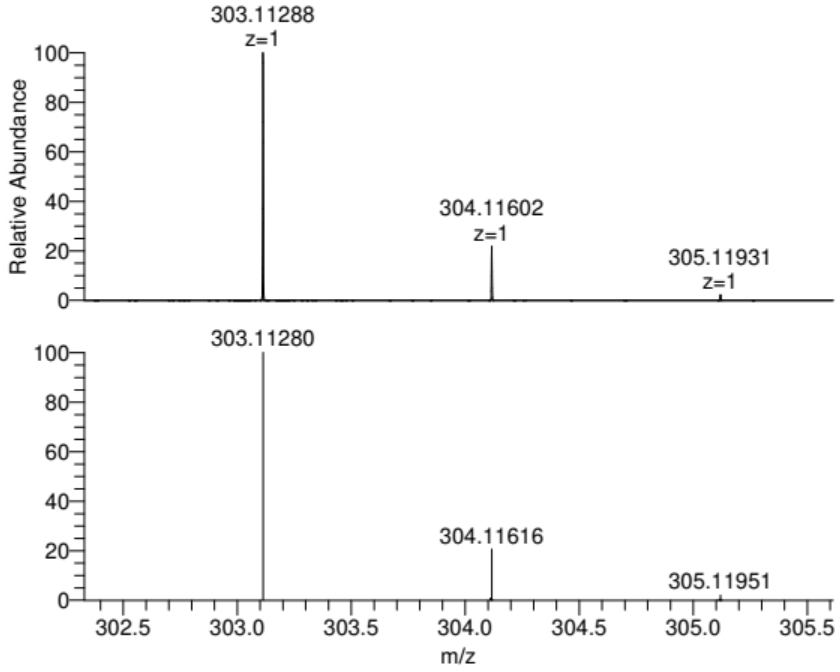

Figure S9. High resolution mass spectra of **NIP**. **NIP**: HRMS (ESI): m/z calcd for [M+H]: 303.11280; found: 303.11288.

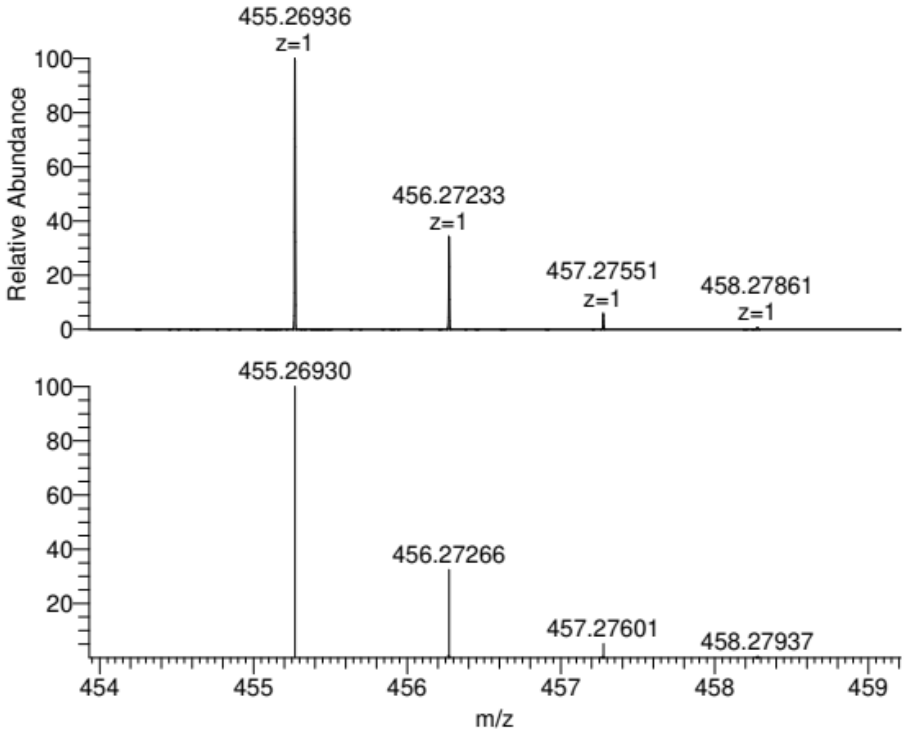

Figure S10. High resolution mass spectra of **NIP**·Br. **NIP**·Br: HRMS (ESI): m/z calcd for [M-Br]: 455.26930; found: 455.26936.

5. Optical Characteristics of NIP·Br in Solution

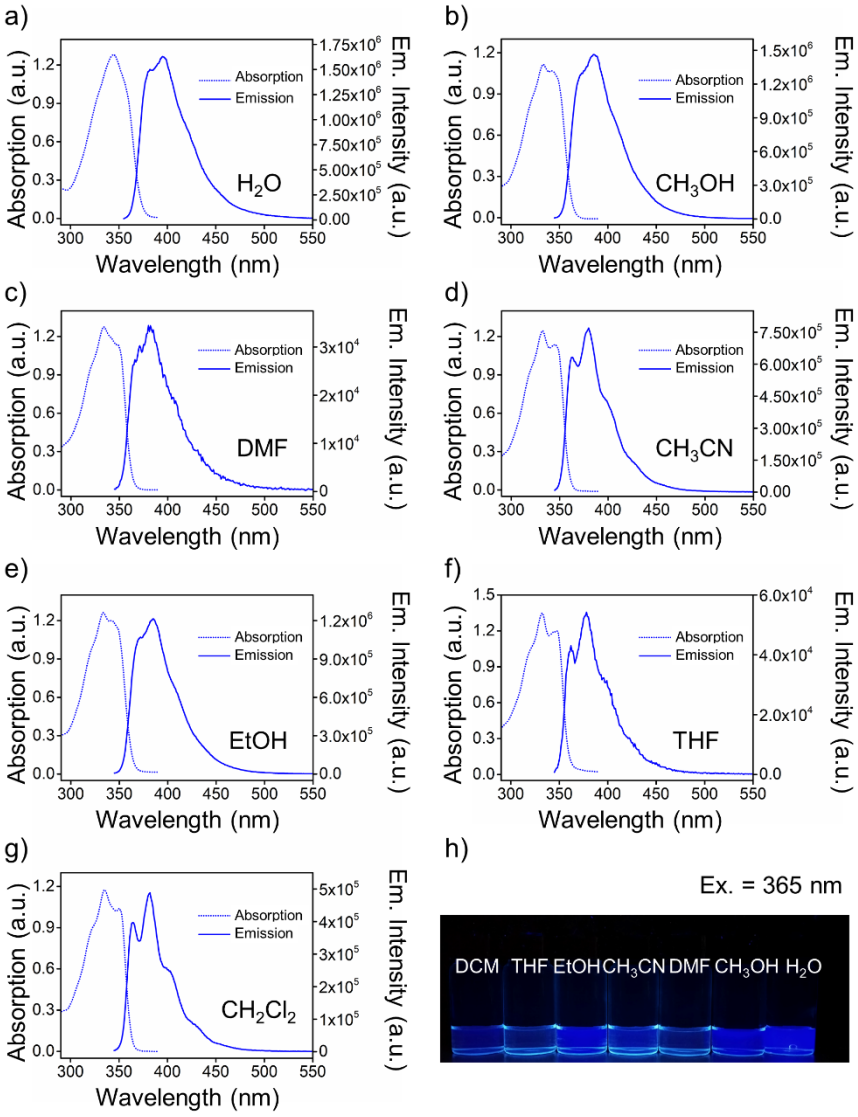

Figure S11. The absorption and emission spectra of a 0.1 mM solution of **NIP**·Br in a) water, b) methanol, c) dimethylformamide, d) acetonitrile, e) ethanol, f) tetrahydrofuran, and g) dichloromethane. h) The fluorescence emission of a 0.1 mM solution of **NIP**·Br in various solvents as visualized under 365 nm UV light irradiation.

Table S1. Photophysical Data for the Excitation Center λ_{max}, Emission Center λ_{max}, Stokes Shift ($\Delta\nu_{St}$), and the Absolute Quantum Yield (Φ) of NIP·Br in Various Solvents

Parameters	CH_2Cl_2	THF	EtOH	CH_3CN	DMF	CH_3OH	H_2O
Polarizability/10^{-24} cm^3 [a]	6.5	7.9	5.1	4.5	7.9	3.3	1.5
Absorption λ_{max}/nm[b]	335	332	334	332	334	333	345
Emission λ_{max}/nm[b]	382	379	386	380	380	386	395
$\Delta\nu_{St}$/cm^{-1} [c]	3673	3745	3966	3804	3624	4123	3670
Φ[d]	0.036	0.018	0.087	0.065	0.008	0.134	0.157

[a] Calculated using ACD/Labs Percepta Platform - Physchem Module, version 2018.1, Advanced Chemistry Development, Inc. Toronto, ON, Canada, www.acdlabs.com, 2019. [b] All spectra in solution were measured using a 1 cm path length quartz cuvette at a concentration of 1 × 10^{-4} M at 298 K. [c] $\Delta\nu_{St} = \nu Abs_{max} - \nu Em_{max}$. [d] Φ = Absolute fluorescence quantum yield obtained using an integrating sphere.

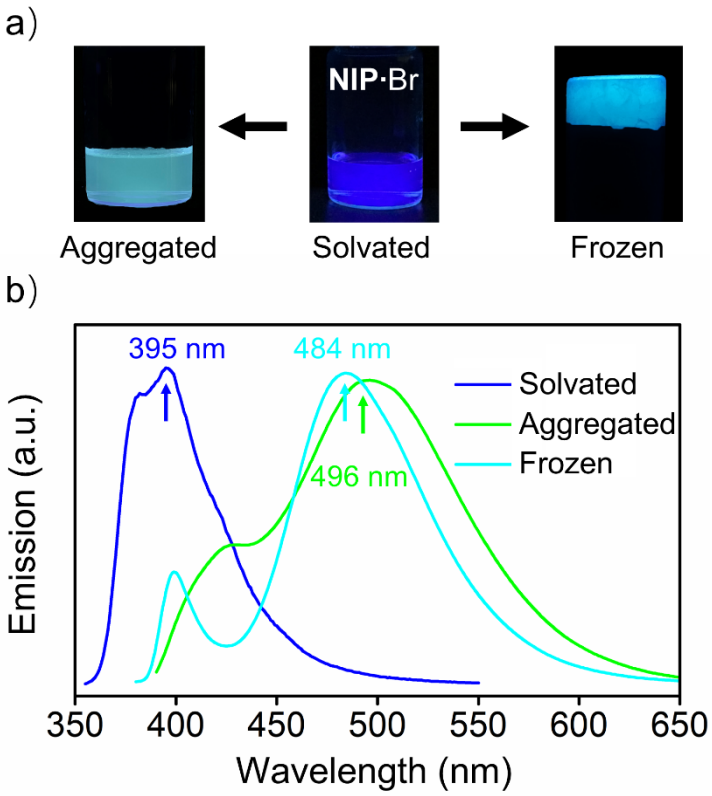

Figure S12. a) Photographs of saturated aqueous solutions of **NIP**·Br exhibiting a visible bathochromic shift upon freezing (right) and aggregation (left) achieved by the increase of the ionic strength of solution with the addition of sodium chloride. b) Emission spectra of **NIP**·Br under the solvated, aggregated, and frozen state.

6. Solid State Fluorescence Hydrochromism of NIP·Br

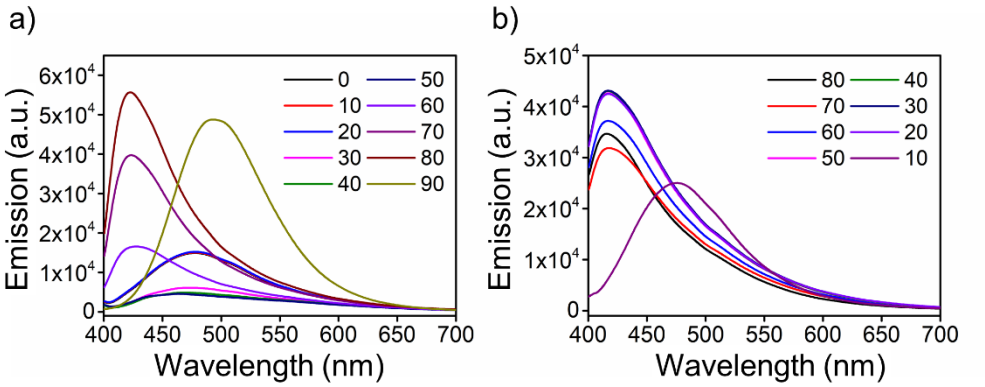

Figure S13. Fluorescence emission spectra of **NIP**·Br powder with a) increasing relative humidity from 0 to 90% and b) decreasing relative humidity from 80 to 10%.

Table S2. Weight % water adsorption and desorption as a function of increasing and decreasing relative humidity as measured by dynamic vapor sorption gravimetry at 298 K for powdered samples of NIP·Br.

Relative Humidity (%)	Water Absorption (%)
0	0
10	0.23
20	0.45
30	0.88
40	1.74
50	2.13
60	4.27
70	4.47
80	5.29
90	8.35
80	6.29
70	4.95
60	4.46
50	4.29
40	4.19
30	4.09
20	3.98
10	0.51

7. CIE Chromaticity Diagram

a)

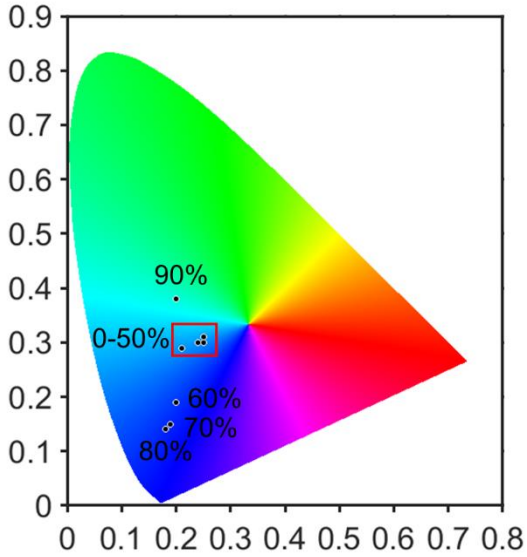

RH (%)	Coordinate
0	(0.21, 0.29)
10	(0.21, 0.29)
20	(0.21, 0.29)
30	(0.24, 0.30)
40	(0.25, 0.31)
50	(0.25, 0.30)
60	(0.20, 0.19)
70	(0.19, 0.15)
80	(0.18, 0.14)
90	(0.20, 0.38)

b)

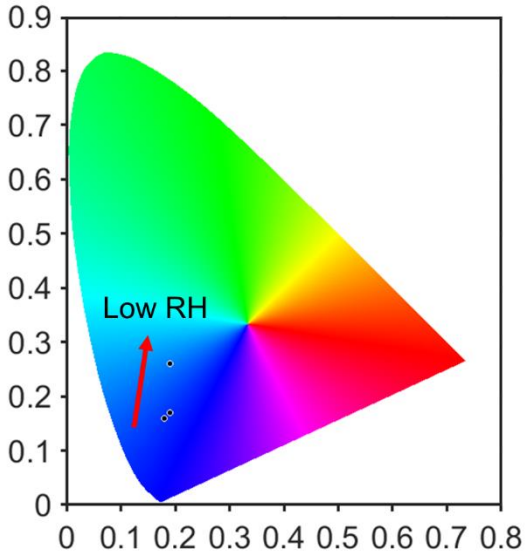

RH (%)	Coordinate
80	(0.18, 0.16)
70	(0.19, 0.17)
60	(0.19, 0.17)
50	(0.19, 0.17)
40	(0.19, 0.17)
30	(0.19, 0.17)
20	(0.19, 0.17)
10	(0.19, 0.26)

Figure S14. CIE chromaticity diagrams (left) of a powdered sample of **NIP**·Br under a) the increasing relative humidity from 0 to 90% and b) decreasing relative humidity from 80 to 10%. The corresponding CIE coordinates of **NIP**·Br for each relative humidity are shown to right of the CIE chromaticity diagrams.

8. Emission Spectra as a Function of Time and Relative Humidity

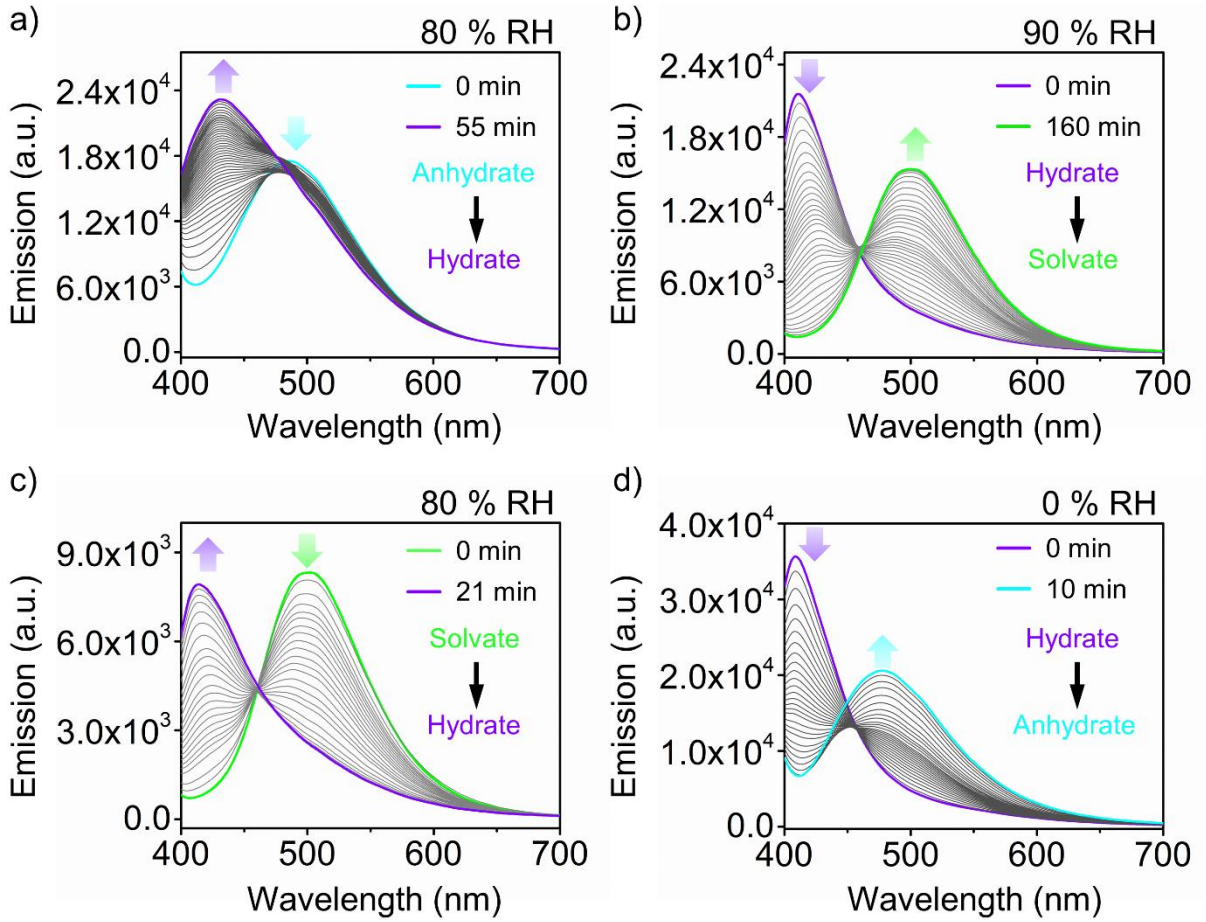

Figure S15. Overlaid emission spectra of a powdered sample of **NIP**·Br measured at different time intervals during conversion from a) its anhydrate state (cyan trace) to its hydrate state (purple trace) while housed within a humidity chamber maintained at 80% RH, b) its monohydrate state to its solvate state (green trace) while exposed to 90% RH, c) its solvate state back to its monohydrate state while exposed to 80% RH, and d) it hydrate state back to its anhydrate state while exposed to 10% RH.

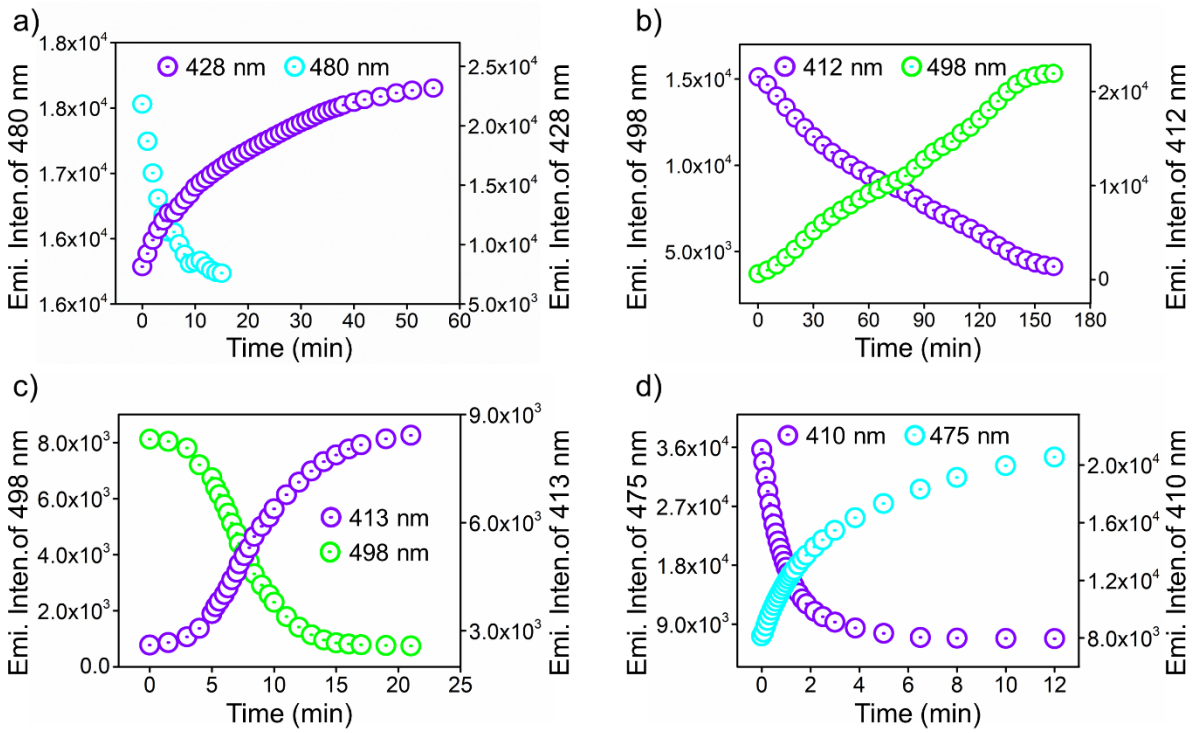

Figure S16. The alteration of emission center intensity of **NIP**·Br powder measured at different time intervals during the conversation of the a) anhydrate state (cyan trace) to the hydrated state (purple trace) within a humidity chamber maintained at 80% relative humidity, during the conversation of the b) hydrated state (purple trace) to the solvated state (green trace) within a humidity chamber maintained at 90% relative humidity, during the conversation of the c) solvated state (green trace) to the hydrated state (purple trace) within a humidity chamber maintained at 80% relative humidity, and during the conversation of the d) hydrated state (purple trace) to the anhydrate state (cyan trace) within a humidity chamber maintained at 0% relative humidity.

9. Dynamic Vapor Sorption/Desorption Gravimetric Analysis

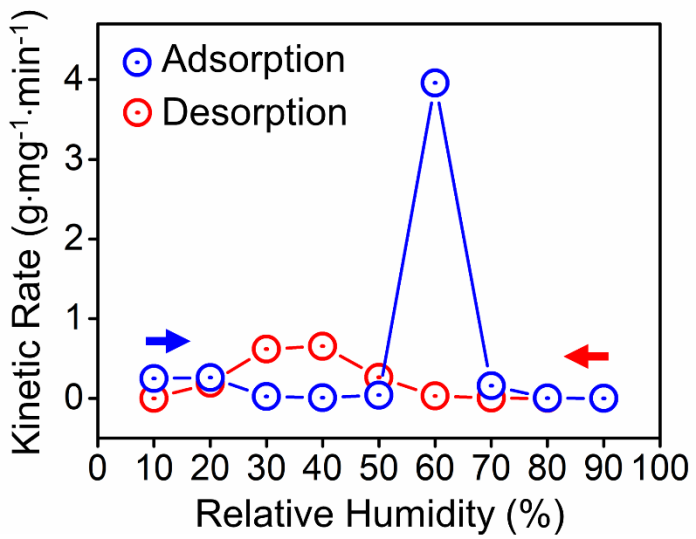

Figure S17. The kinetic rate of water adsorption and desorption by **NIP**·Br as a function of relative humidity

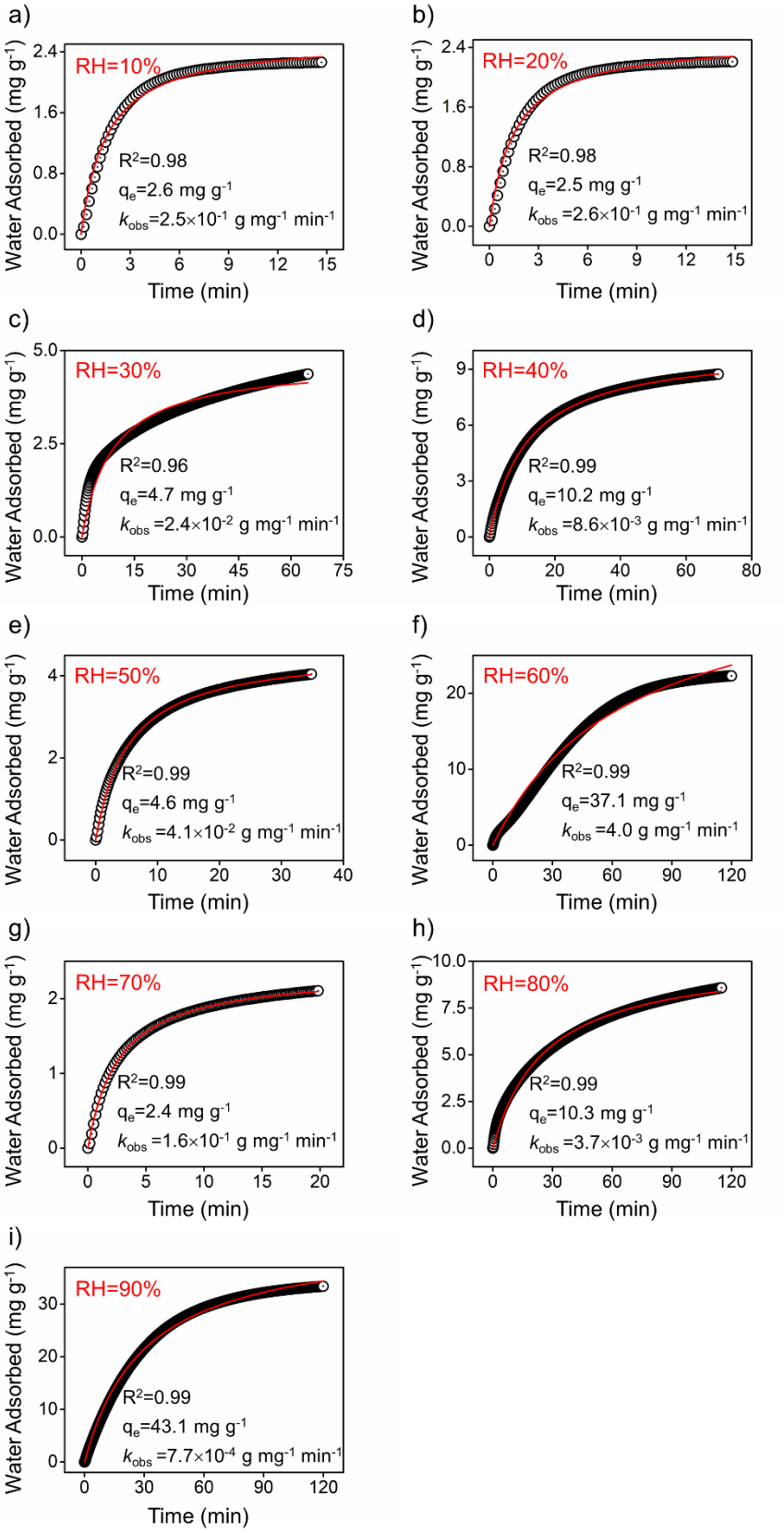

Figure S18. Time-dependent adsorption of water by **NIP**·Br fitted to a pseudo-second order rate equation at different relative humidity values as determined by dynamic vapor sorption/desorption gravimetric analysis.

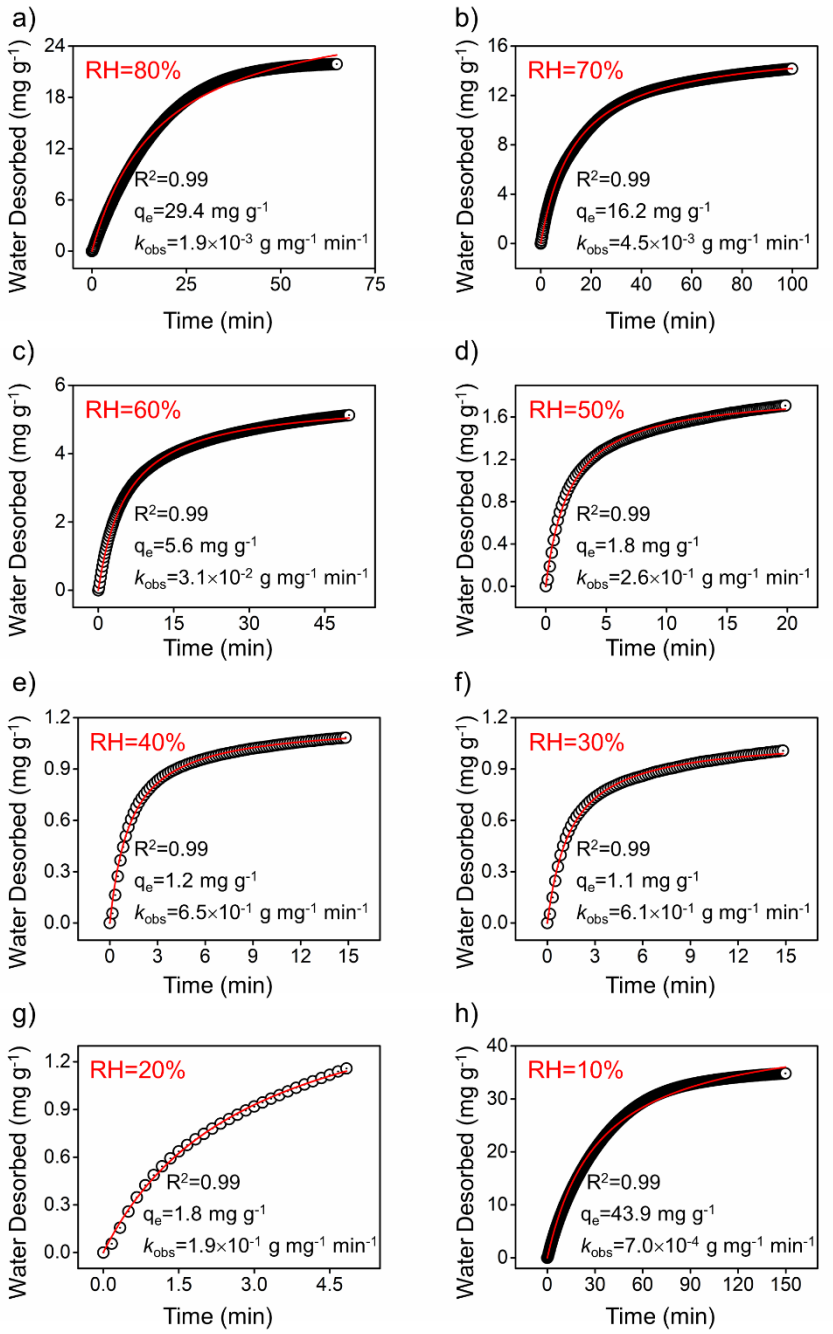

Figure S19. Time-dependent desorption of water by **NIP**·Br fitted to a pseudo-second order rate equation at different relative humidity values as determined by dynamic vapor sorption/desorption gravimetric analysis.